FEBS Letters 514 (2002) 168–174 FEBS 25832

The acidic regions of WASp and N-WASP can synergize with CDC42Hs and Rac1 to induce filopodia and lamellipodia

Katharina Hüfner[a], Barbara Schell[a], Martin Aepfelbacher[b], Stefan Linder[a,*]

[a] *Institut für Prophylaxe und Epidemiologie der Kreislaufkrankheiten, Ludwig-Maximilians-Universität, Pettenkoferstr. 9, 80336 Munich, Germany*
[b] *Max von Pettenkofer-Institut für Medizinische Mikrobiologie, Ludwig-Maximilians-Universität, Pettenkoferstr. 9, 80336 Munich, Germany*

Received 3 December 2001; revised 14 January 2002; accepted 15 January 2002

First published online 14 February 2002

Edited by Amy McGough

Abstract The acidic (A) region of WASp family proteins is thought to represent a high-affinity binding site for Arp2/3 complex without activating properties. Here we show that GST-fused WASp-A and N-WASP-A, but not a WASP-A/W500S mutant, several truncated WASp-A constructs or WAVE1-A can pull down Arp2/3 complex from cell lysates. Significantly, WASp-A and N-WASP-A synergistically trigger formation of filopodia or lamellipodia when coinjected with sub-effective concentrations of V12CDC42Hs or V12Rac1, respectively, into macrophages. The ability of WASp family A region constructs to induce this effect is closely correlated with their ability to bind Arp2/3 complex in vitro. These results imply that (i) Arp2/3 complex is critically involved in filopodia and lamellipodia formation in macrophages and (ii) acidic regions of WASp and N-WASP are not simply binding sites for Arp2/3 complex but can prime it for RhoGTPase-triggered signals leading to actin nucleation.

Key words: Actin cytoskeleton; WASp family protein; Arp2/3 complex; Filopodium; Lamellipodium

1. Introduction

Arp2/3 complex has been implicated in the formation of f-actin structures like lamellipodia [1], podosomes [2], comet tails of *Listeria* [3] (reviewed in [4]) and *Shigella* [5] (reviewed in [4]), and phagocytic uptake structures [6–8].

The human WASp family comprises WASp, N-WASp and three WAVE/Scar isoforms and is thought to link RhoGTPase-mediated signal transduction to actin nucleation via Arp2/3 complex (reviewed in [9–11]). For example, CDC42 has been shown to trigger formation of filopodia [12–14] (reviewed in [11,15]), while Rac mediates formation of lamellipodia/ruffles via WASp family proteins [16,17] (reviewed in [11,15]).

The isolated C-terminal VCA domain of WASp family proteins, containing verprolin-like, central and acidic regions (Fig. 1A), binds both actin and Arp2/3 complex and activates Arp2/3 complex in vitro and in vivo [18–21]. Binding of monomeric actin is mostly achieved through the V region, while both the C and A regions mediate binding to Arp2/3 complex [21,22].

Binding to members of the Wiskott–Aldrich syndrome protein (WASp) family transforms the basally inactive Arp2/3 complex into a highly efficient nucleator of actin filaments that grow from their barbed ends (reviewed in [9–11]). In this context, the C-terminal acidic (A) region of WASp family proteins is thought to represent a high-affinity binding site for Arp2/3 complex without activating properties ([18,19], reviewed in [9]).

Recently, WASp-VC was shown to be the minimal necessary region for Arp2/3 complex activation in vitro and in cells [22]. Furthermore, GST fusions of the CA or C regions lead to actin aggregation in cells upon microinjection [22]. This leaves the Arp2/3 complex binding A region of WASp as a potential tool to probe Arp2/3 complex involvement in cellular processes. This study was therefore set up to explore in greater detail the Arp2/3 binding abilities of acidic regions of WASp family proteins (Fig. 1B).

2. Materials and methods

2.1. Cell isolation and culture

Human peripheral blood leukocytes were isolated by centrifugation of heparinized blood in Ficoll (Biochrom, Berlin, Germany). Monocytic cells were isolated with magnetic anti-CD14 antibody beads and an MS+ separation column (Miltenyi Biotec, Auburn, CA, USA) according to the manufacturer's instructions and seeded onto Cellocate coverslips (Eppendorf, Hamburg, Germany) at a density of 5×10^4 per coverslip. Cells were cultured in RPMI containing 20% autologous serum at 37°C, 5% CO_2 and 90% humidity. Medium was changed every 3–4 days.

2.2. Generation of constructs and protein expression

WASp constructs were created by cloning PCR-generated inserts (in the case of WASp-CA and WASp-A constructs) or commercially synthesized oligonucleotides (MWG Biotech, Germany) in the case of WASp-A13, WASp-A11, WASp-A9, WASp-A7 and WASpA/W500S into the *Bam*HI and *Eco*RI sites of vector pGEX-2T (Amersham Pharmacia Biotech, Uppsala, Sweden), as in part described earlier [2,23]. Vectors for expression of V12CDC42Hs and V12Rac1 were kind gifts of Dr. A. Hall (London, UK). Proteins were expressed as glutathione *S*-transferase (GST) fusion proteins in *Escherichia coli* as described [23]. When indicated, GST was removed by thrombin cleavage, according to the manufacturer's instructions. For microinjection, proteins were dialyzed against microinjection buffer (50 mM Tris–HCl, 150 mM NaCl, 5 mM $MgCl_2$), concentrated in Centricon filters (Millipore, Bedford, MA, USA), shock-frozen and stored at −80°C. Purity was tested by SDS–PAGE and Coomassie staining. For anisotropy experiments, GST fusions of the WASp acidic region were purified by FPLC, as described [22].

2.3. GST pull down assay and immunoblotting

GST pull downs were prepared as described previously [2]. Briefly, a total of 3×10^6 cells cultured for 5–14 days in six well plates (Nunc) at a density of 1×10^6 cells/well were washed in ice-cold phosphate-buffered saline (PBS) and lysed by the addition of 200 μl/well RIPA

*Corresponding author. Fax: (49)-89-5160 4382.
E-mail address: stefan.linder@klp.med.uni-muenchen.de (S. Linder).

0014-5793/02/$22.00
PII: S0014-5793(02)02358-X

buffer (20 mM Tris–HCl, pH 8.0, 1 mM EDTA, 1% Triton X-100, 75 mM $NaCl_2$) containing protease inhibitors. After centrifugation (15 000 rpm, 15 min, 4°C), aliquots of the supernatant were added to glutathione Sepharose beads, previously incubated for 1 h with 50 μg of GST fusion proteins. Beads were incubated with lysate for 30 min at 4°C, washed extensively in RIPA buffer and pelleted. 100 μl of SDS sample buffer was added, and an aliquot was run on a 12.5% SDS gel. Western blots were prepared as described previously [23]. Arp2/3 complex was detected by using polyclonal anti-ARPC1 and -ARPC2 antibodies [2]. Secondary antibody was horseradish peroxidase-conjugated (Amersham Pharmacia Biotech). No binding of the screened proteins was detected when GST alone was bound to beads.

2.4. Fluorescence anisotropy measurements

Experiments were conducted as described elsewhere [22]. Briefly, 0.1 μM of rhodamine-labeled WASp VCA (without GST), 0.1 μM Arp2/3 complex and varying concentrations of binding partners were incubated in 20 nM imidazole, pH 7.0, 50 mM KCl, 1 mM $MgCl_2$, 1 mM EGTA, 0.025% Thesit (Roche Molecular Biochemicals, Basel, Switzerland) for 2 min at room temperature. Fluorescence anisotropy was measured in an Alpha-scan spectrofluorimeter (Photon Technologies International) at 552 nm excitation at 574 nm emission and plotted in arbitrary units. Dissociation equilibrium constants (K_d) were calculated as described earlier [21]. GST controls showed no effect in the anisotropy measurements. Arp2/3 complex was prepared from bovine thymus as described [24].

2.5. Microinjection of proteins

Cells for microinjection experiments were cultured for 5–8 days. Microinjection was performed using transjector 5246 (Eppendorf) and a Compic Inject micromanipulator (Cell Biology Trading, Hamburg, Germany). GST fusions of WASp C-terminal regions, GST-V12CDC42 and GST-free V12Rac were injected at the indicated concentrations. Cells were incubated for 1 h post injection. Control injections were performed with GST alone. Injected cells were identified by detection of coinjected rat IgG (5 mg/ml) with FITC-labeled goat anti-rat IgG antibody (both Dianova, Hamburg, Germany).

2.6. Immunofluorescence microscopy

For actin and Arp2/3 complex staining, cells were grown on coverslips for 5–8 days and microinjected when indicated. Samples were then fixed for 10 min in PBS solution containing 3.7% formaldehyde and permeabilized for 5 min in ice-cold acetone. Background fluorescence was reduced by incubating coverslips with 5% human serum and 5% normal goat serum (both Dianova) in PBS. Actin was detected with Alexa 568-labeled phalloidin (Molecular Probes, Leiden, The Netherlands) or with monoclonal antibody MAB1501 (Chemicon, Temecula, CA, USA), Arp2/3 complex was detected by staining with anti-ARPC2 antibody [2]. Secondary antibody was Alexa 488-labeled goat anti-rabbit (Molecular Probes). Coverslips were mounted in Mowiol (Calbiochem, Schwalbach, Germany), containing *p*-phenylenediamine (Sigma, Deisenhofen, Germany) as anti-fading reagent, and sealed with nail polish. Images were obtained either by confocal laser scanning microscopy (Leica, Wetzlar, Germany) or with a spot digital camera (Leica).

3. Results and discussion

To map residues of the 15 aa WASp A region necessary for interaction with Arp2/3 complex, a series of N-terminally truncated constructs fused to the C-terminus of GST were created and named accordingly WASp-A13, WASp-A11, WASp-A9 and WASp-A7 (Fig. 1C). We first assessed the ability of these constructs to pull down Arp2/3 complex from macrophage lysates (Fig. 2A). WASp-A was able to pull down Arp2/3 complex, as described [2], while shorter constructs bound with decreasing efficiency. WASp-A11 displayed only minimal ability to pull down Arp2/3 complex, while WASp-A7 showed no interaction in this assay (Fig. 2A). Decreasing ability to pull down Arp2/3 complex was reflected by decreasing affinity for Arp2/3 complex in anisotropy assays. For example, WASp-A15 bound Arp2/3 complex with a K_d of 1.0 μM (Fig. 2C [22]), while WASp-A9 bound with a K_d of 4.0 μM (Fig. 2D). As positive and negative controls respectively, we used construct WASp-CA (Fig. 1A), comprising all known binding sites for Arp2/3 complex in the VCA domain [21,22], and construct WASp-A/W500S (Fig. 1C) carrying a point mutation previously shown to drastically reduce the affinity of WASp VCA for Arp2/3 complex [21]. WASp-CA bound Arp2/3 complex efficiently, as shown earlier [22] (Fig. 2A), while WASp-A/W500S displayed no detectable interaction with Arp2/3 complex in this assay (Fig. 2A). We conclude from these experiments that, apart from the previously identified W500 amino acid residue, also the presence of the four N-terminal amino acid residues of the WASp A region (aa 488–491) is critical for interaction with Arp2/3 complex in vitro.

The A regions of WASp and N-WASP are highly homologous (11 identical amino acids; Fig. 1B), while those of

Fig. 1. Domain organization of WASp, GST fusion constructs of WASp C-terminus and comparison of acidic regions of WASp family proteins. A: Domain organization of WASp: WASp homology domain 1 (WH1), basic domain (B), GTPase binding domain (GBD), polyproline domain, C-terminal domain (containing verprolin-like (V), central C-terminal (C) and acidic (A) regions). Numbers indicate first and last amino acids of proteins. B: Comparison of acidic regions of WASp, N-WASP and WAVE1. C: Truncated or mutated forms of the WASp A region used in this study.

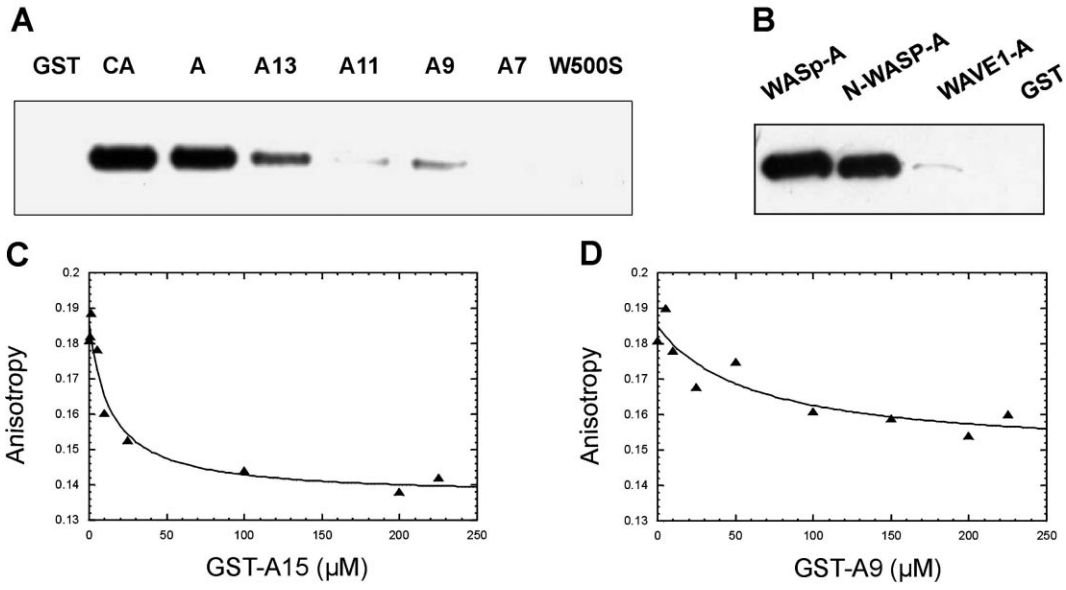

Fig. 2. Arp2/3 complex binding of GST fusions containing C-terminal acidic peptides of WASp family proteins. Western blots of GST pull down experiments using (A) a series of N-terminally truncated or mutated constructs of WASp C-terminus or (B) constructs of acidic regions of WASp family proteins, probed with ARPC1-specific antibody. Denominations of polypeptides are given above each lane. Anisotropy measurement of binding to Arp2/3 complex by WASp-A (C) and WASp-A9 (D) constructs. Increasing amounts of the respective construct were allowed to compete with rhodamine-labeled (GST-free) WASp VCA. Decrease in anisotropy indicates successful competition by the respective construct.

WAVE proteins are clearly more divergent (7 homologous amino acids in WAVE1-A compared to WASp-A; Fig. 1B). A GST fusion of the N-WASP acidic region, N-WASP-A (Fig. 1B), showed comparable ability to WASp-A to pull down Arp2/3 complex from macrophage lysates (Fig. 2B), while the respective WAVE1 construct, WAVE1-A (Fig. 1C), was barely able to do so (Fig. 2B). The high identity of WASp and N-WASp acidic regions is therefore also mirrored by a functional similarity in Arp2/3 complex binding. In contrast, the acidic region of WAVE1 seems to be necessary [18,25], but is clearly not sufficient for Arp2/3 complex binding.

We went on to investigate whether formation of specific actin structures in cells is dependent on Arp2/3 complex. Microinjection of primary human macrophages with the constitutively active GTPase mutants V12CDC42Hs (0.2 μg/μl) or V12Rac1 (0.2 μg/μl) leads to formation of filopodia or lamellipodia/ruffles, respectively ([23] and Linder, unpublished). The latter effect is mostly associated with cell spreading. When microinjected at values below the effective concentrations, neither the GTPase mutants (V12CDC42: 0.1 μg/μl; V12Rac: 0.1 μg/μl; Fig. 3A,B) nor WASp-A (4 μg/μl; Fig. 3C) or N-WASP-A (4 μg/μl; Fig. 3F) had a discernible effect on the actin cytoskeleton (cells showing filopodia: V12CDC42, 10 ± 9%; WASp-A, 12 ± 2%; N-WASp-A, 12 ± 4%; cells showing ruffles: V12Rac, 3 ± 3%; WASp-A, 0 ± 0%; N-WASp-A, 0 ± 0%; Fig. 4). However, coinjection of WASp-A or N-WASp-A with either one of the constitutively active GTPase mutants, all proteins at sub-threshold concentrations, dramatically enhanced formation of filopodia or ruffles (Fig. 3D,E,G,H). The respective phenotype was dependent on the GTPase mutant: coinjection with V12CDC42Hs resulted in filopodia formation (cells showing filopodia: V12CDC42+WASp-A, 97 ± 6%; V12CDC42+N-WASp-A, 96 ± 4%; Figs. 3D,G and 4), while coinjection with V12Rac triggered formation of ruffles and cell spreading (cells showing ruffles: V12Rac+WASp-A, 91 ± 2%; V12Rac+N-WASp-A, 94 ± 5%; Figs. 3E,H and 4). In this respect, the A regions of WASp and N-WASp were interchangeable.

In contrast, coinjection of the GTPase mutants with WAVE1-A failed to elicit any discernible effect on the actin cytoskeleton (cells showing filopodia: V12CDC42+WAVE1-A, 8 ± 2%; cells showing ruffles: V12Rac+WAVE1-A, 6 ± 7%; Fig. 4). In addition, WASp-A13 was able to stimulate formation of filopodia or ruffles in coinjection experiments (Fig. 4), although to a lesser degree compared to WASp-A, while all shorter constructs of the WASp acidic region failed to do so (Fig. 4 and not shown). Coinjection of GTPase constructs with the WASp-A/W500S mutant resulted in a marked decrease in both filopodia and ruffle formation compared to coinjections with WASp-A (cells showing filopodia: V12CDC42+WASp-A/W500S, 12 ± 8%; cells showing ruffles: V12Rac+WASp-A/W500S, 19 ± 5%; Fig. 4). Additionally, coinjection of WASp-CA (Fig. 1A) stimulated filopodia or ruffle formation even at concentrations of 0.5 μg/μl (not shown). This requirement for lower effective concentrations fits well with WASp-CA showing a 10-fold higher affinity for Arp2/3 complex (K_d: 0.1 μM [22]) than WASp-A (K_d: 1 μM).

Formation of filopodia or ruffles in microinjected cells was often accompanied by disruption of podosomes, actin-rich adhesion structures controlled by WASp [2,23]. Therefore, regulation of podosomes apparently differs from that of filopodia and lamellipodia. It seems that Arp2/3 complex bound to WASp family A region constructs is not incorporated into podosomes [2], but can be used effectively by GTPase-triggered pathways to induce filopodia and ruffles. These signals may involve e.g. the CDC42-IRSp53-Mena pathway recently shown to be important for filopodia formation in Swiss 3T3 cells [26].

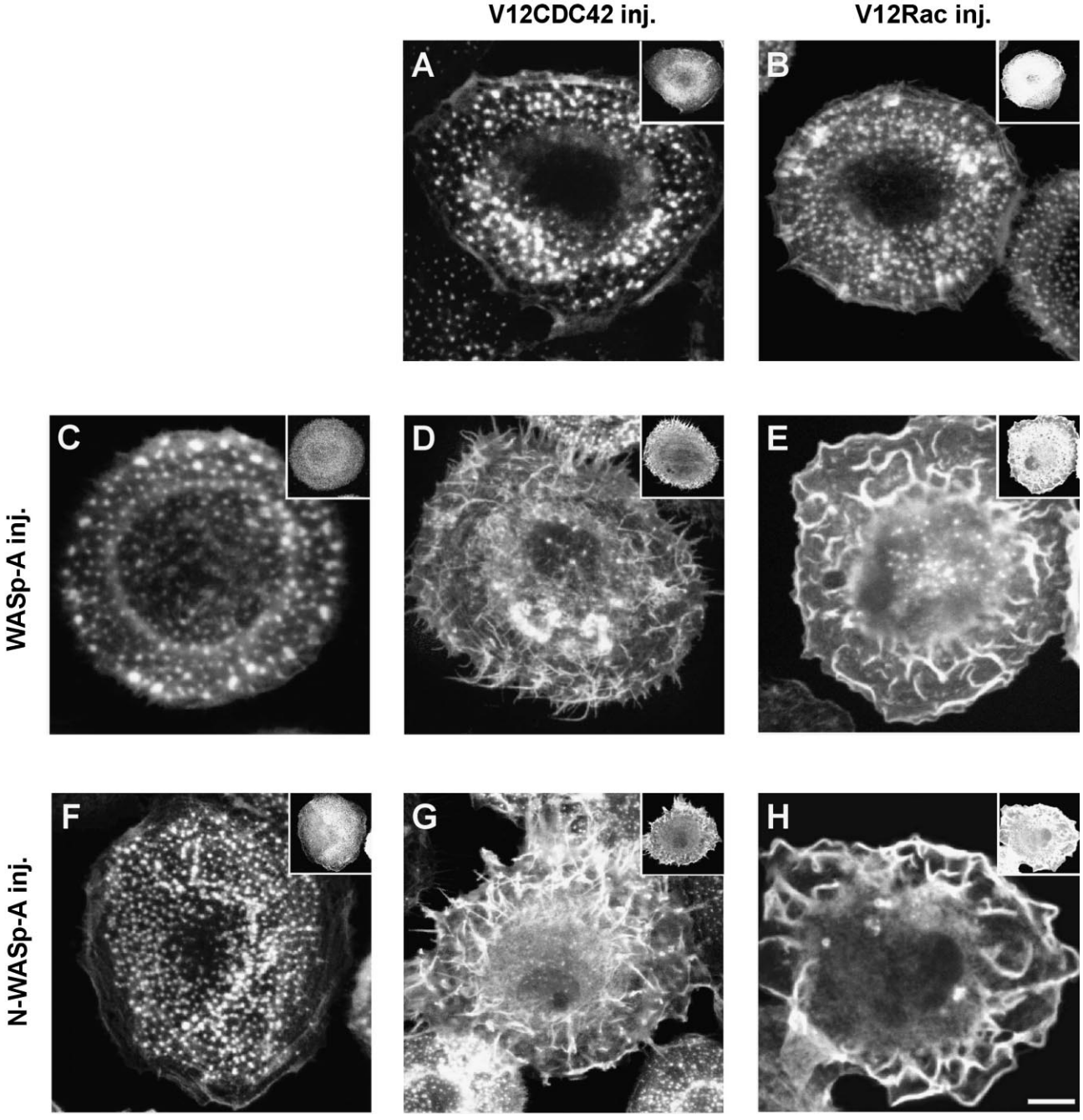

Fig. 3. Coinjection of WASp-A or N-WASp-A with constitutively active GTPase mutants has a synergistic effect on filopodia and lamellipodia formation. A–H: Confocal laser scanning micrographs of primary human macrophages stained for f-actin 1 h post injection. Insets show staining of rat IgG used as an injection marker. V12CDC42 (A) and V12Rac (B) were injected at 0.1 μg/μl. WASp-A (C) and N-WASP-A (F) were injected at 4 μg/μl. No effect on the actin cytoskeleton was observed at these concentrations. Coinjection of V12CDC42 with WASp-A (D) or N-WASp-A (G) at these concentrations led to prominent formation of filopodia, while coinjection of V12Rac with WASp-A (E) or N-WASP-A (H) led to formation of ruffles and cell spreading. White bar indicates 12 μm for E and H and 10 μm for all others.

In sum, we assessed the Arp2/3 complex binding abilities of WASp family acidic constructs in vitro and in vivo. The acidic regions of WASp and N-WASp, but not of WAVE1, were found to interact efficiently with Arp2/3 complex in vitro. The four N-terminal amino acid residues of WASp-A are crucial for this effect. Significantly, we observed a synergistic effect in the formation of filopodia and ruffles when GST fusions of the acidic regions of WASp or N-WASP were coinjected into macrophages with constitutively active mutants of CDC42Hs or Rac1. Coinjection with WASp-A13 also showed a synergistic effect on filopodia or ruffle formation, although to a less marked degree compared to the full-length WASp-A. Coinjections of GTPases with all shorter constructs of the WASp acidic region as well as the WASp-A/W500S construct or the WAVE-1A construct led to no significant increase in actin structure formation. The ability of WASp family A region constructs to induce actin structure formation thus closely correlated with their ability to bind actin nucleat-

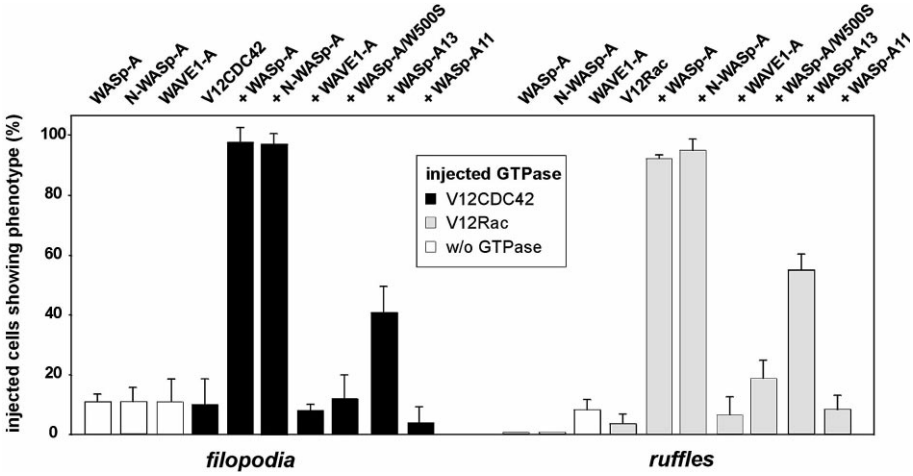

Fig. 4. Evaluation of actin structure formation in primary human macrophages microinjected with WASp family acidic constructs and/or constitutively active GTPase mutants. White columns: injection of WASp family acidic construct without GTPase mutant; black columns: injection of V12CDC42 (0.1 μg/μl); gray columns: injection of V12Rac (0.1 μg/μl), '+' indicates coinjection with respective WASp family acidic region construct (4 μg/μl). Denominations of microinjected polypeptides are given above each column. Values for cells showing actin structure formation are given as mean percentage ± S.D. Filopodia formation: WASp-A, 12 ± 2%; N-WASp-A, 12 ± 4%; WAVE1-A, 12 ± 7%; V12CDC42, 10 ± 9%; V12CDC42+WASp-A, 97 ± 6%; V12CDC42+N-WASp-A, 96 ± 4%; V12CDC42+WAVE1-A, 8 ± 2%; V12CDC42+WASp-A/W500S, 12 ± 8%; V12CDC42+WASp-A13, 41 ± 10%; V12CDC42+WASp-A11, 3 ± 6%. Ruffle formation: WASp-A, 0 ± 0%; N-WASp-A, 0 ± 0%; WAVE1-A, 8 ± 4%; V12Rac, 3 ± 3%; V12Rac+WASp-A, 91 ± 2%; V12Rac+N-WASp-A, 94 ± 5%; V12Rac+WAVE1-A, 6 ± 7%; V12Rac+WASp-A/W500S, 19 ± 5%; V12Rac+WASp-A13, 53 ± 7%; V12Rac+WASp-A11, 8 ± 5%. For each value, three times 30 cells microinjected with the respective construct were evaluated.

ing Arp2/3 complex in vitro. Therefore, Arp2/3 complex binding is most probably a prerequisite for the observed effects, which is also indicated by the recruitment of Arp2/3 complex to the induced structures (Fig. 5).

To elucidate the mechanism by which the observed structures are induced, we studied the distribution of WASp, N-WASP and WAVE in uninjected cells and in cells coinjected with WASp-A with $CDC42^{V12}$/Rac^{V12} (not shown). We find that, although the podosomal localization of WASp is destroyed upon microinjection of WASp-A with $CDC42^{V12}$/Rac^{V12}, there is no significant colocalization of endogenous WASp with either filopodia or ruffles. In a previous study, we also found no indication for an interaction of WASp-A with endogenous WASp in vitro [22]. On the other hand, N-WASp and WAVE localize to newly formed filopodia or ruffles, respectively. Ultimately, we cannot rule out that WASp-A or endogenous WASp plays a role in the generation of these structures. However, according to our data it is likely that filopodia and lamellipodia are induced and localized by the pathways CDC42-N-WASP-Arp2/3 complex and Rac-WAVE-Arp2/3 complex, respectively. In this scenario, WASp-A would only induce 'priming' of Arp2/3 complex, which would explain the high efficiency in structure formation, while the generation of specific structures as well as their localization would not be based on WASp-A activity.

In a recent paper, Zalevsky et al. [27] show that in a chimera of the WAVE1 C-terminal domain, replacement of the acidic region of WAVE1 with the acidic region of N-WASp results in a 20-fold increase in actin nucleating ability. This fits well with our data that, in contrast to WASp-A and N-WASP-A, WAVE1-A is not able to bind Arp2/3 complex efficiently in vitro or to induce actin structures upon coinjection of WASpA with $CDC42^{V12}$/Rac^{V12}. It is not yet clear where the 'priming' step proposed in the present paper would fit in the actin nucleation model presented by Zalevsky et al. [27]. It may occur directly upon binding of WASp/N-WASp to Arp2/3 complex but also at a later step.

Our results imply that (i) Arp2/3 complex is critically involved in the generation of both filopodia and ruffles in primary human macrophages and (ii) the acidic regions of WASp and N-WASP are not simply high-affinity binding sites for Arp2/3 complex. It may be that these regions induce a 'priming' step which does not lead to full activation but to heightened susceptibility of Arp2/3 complex for GTPase-triggered signals to induce actin polymerization. The existence of additional activation steps in actin nucleating pathways has already been speculated upon [21]. Our results give the first indication at the cellular level that at least one such additional step may in fact exist. The acidic region constructs used in this study may also be helpful tools in further addressing this issue and also whether actin-dependent processes in cells are Arp2/3 complex-dependent.

Acknowledgements: We thank Peter C. Weber, Jürgen Heesemann and Thomas D. Pollard for continuous support, Barbara Böhlig for expert technical assistance and Henry N. Higgs and Jean-Baptiste Marchand for help with anisotropy measurements. This work was supported by grants of the Deutsche Forschungsgemeinschaft (SFB 413, Ae 11) to S.L. and M.A. and by August Lenz Stiftung to S.L. This work is part of the doctoral thesis of Katharina Hüfner at the LMU München, Germany.

References

[1] Svitkina, T.M. and Borisy, G.G. (1999) J. Cell Biol. 5, 1009–1026.
[2] Linder, S., Higgs, H.N., Hüfner, K., Schwarz, K., Pannicke, U. and Aepfelbacher, M. (2000) J. Immunol. 165, 221–225.
[3] May, R.C., Hall, M.E., Higgs, H.N., Pollard, T.D., Chakraborty, T., Wehland, J., Machesky, L.M. and Sechi, A.S. (1999) Curr. Biol. 9, 759–762.
[4] Cossart, P. (2000) Cell Microbiol. 2, 195–205.
[5] Egile, C., Loisel, T.P., Laurent, V., Li, R., Pantaloni, D., Sansonetti, P.J. and Carlier, M.F. (1999) J. Cell Biol. 146, 1319–1332.

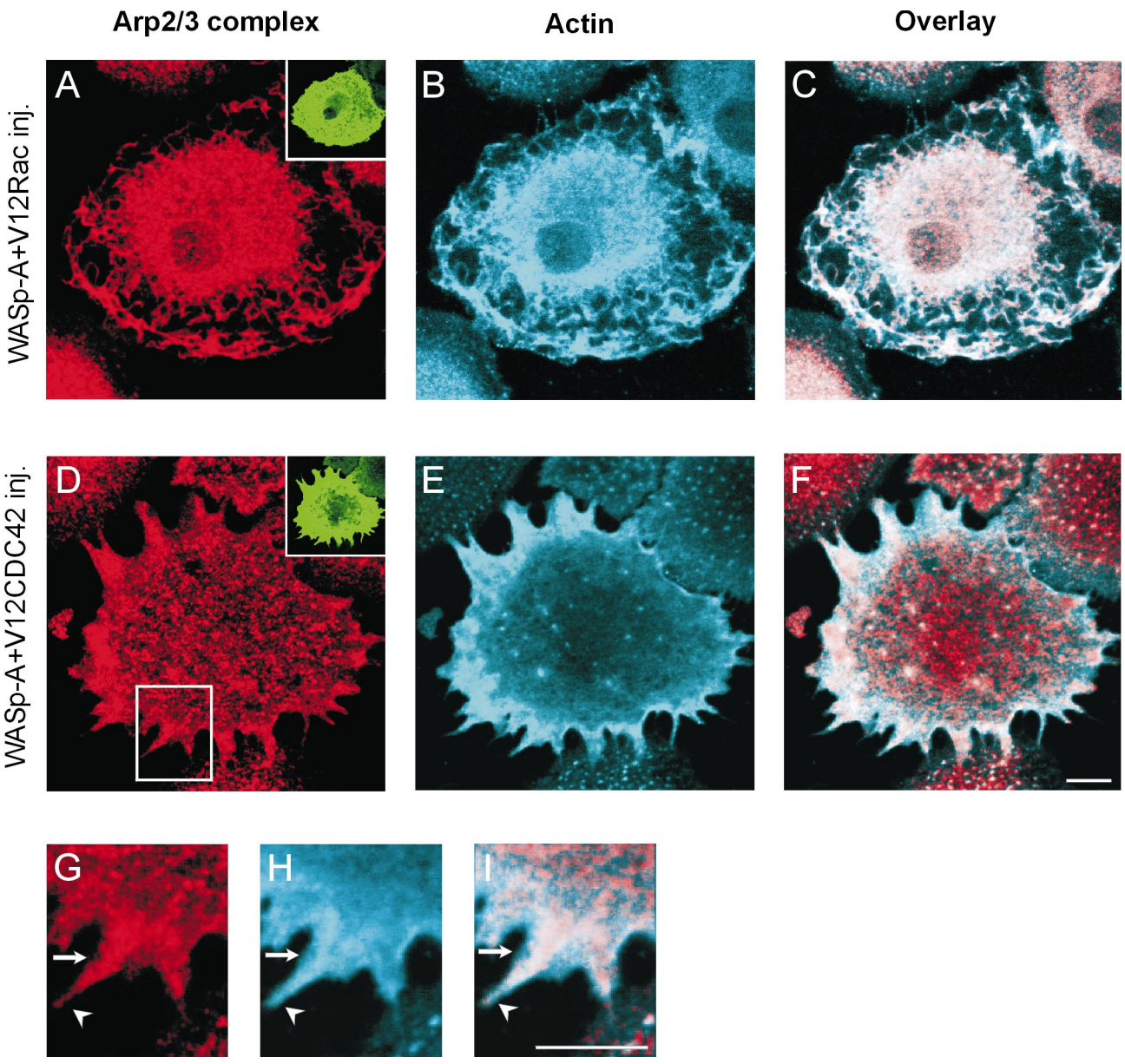

Fig. 5. Arp2/3 complex localizes to actin structures induced by coinjection of WASp acidic regions and constitutively active GTPase mutants. Confocal laser scanning micrographs of 7 day old macrophages microinjected with V12Rac+WASp-A (A–C), or V12CDC42Hs+WASp-A (D–I). Pictures were gained by superimposition of each time three (A–C) or two (D–I) confocal sections with a scanning difference of 1–2 μm. Red color, Arp2/3 complex stained with anti-ARPC2 antibody (A,D,G), blue color, actin stained with anti-actin antibody (B,E,H), overlay of a and b (C), of d and e (F) and of g and h (I), pink color indicates colocalization. Insets in A,D show staining of coinjected rat IgG used as injection marker. G–I show details of D–F, with white box in D indicating the magnified part of the respective panels. White arrows indicate the basis of a filopodium with accumulations of Arp2/3 complex and f-actin, white arrowheads indicate tip of filopodium with accumulations of f-actin but not of Arp2/3 complex. White bars indicate 10 μm for all panels of the same sizes.

[6] May, R.C., Caron, E., Hall, A. and Machesky, L.M. (2000) Nature Cell Biol. 2, 246–248.
[7] Wiedemann, A., Linder, S., Grassl, G., Albert, M., Autenrieth, I. and Aepfelbacher, M. (2001) Cell Microbiol. 3, 693–702.
[8] Linder, S., Heimerl, C., Fingerle, V., Aepfelbacher, M. and Wilske, B. (2001) Infect. Immun. 69, 1739–1746.
[9] Higgs, H.N. and Pollard, T.D. (1999) J. Biol. Chem. 274, 32531–32534.
[10] Mullins, R.D. (2000) Curr. Opin. Cell Biol. 12, 97–103.
[11] Takenawa, T. and Miki, H. (2001) J. Cell Sci. 114, 1801–1807.
[12] Nobes, C.D. and Hall, A. (1995) Cell 81, 53–62.
[13] Miki, H., Sasaki, T., Takai, Y. and Takenawa, T. (1998) Nature 391, 93–96.
[14] Castellano, F., Montcourrier, P., Guillemot, J-C., Gouin, E., Machesky, L.M., Cossart, P. and Chavrier, P. (1999) Curr. Biol. 9, 351–360.
[15] Svitkina, T.M. and Borisy, G.G. (1999) Trends Biol. Sci. 24, 432–436.
[16] Ridley, A.J., Paterson, H.F., Johnston, C.L., Diekmann, C.L. and Hall, A. (1992) Cell 70, 401–410.
[17] Machesky, L.M. and Insall, R.H. (1998) Curr. Biol. 8, 1347–1356.
[18] Machesky, L.M., Mullins, D.M., Higgs, H.N., Kaiser, D.A., Blanchoin, L., May, R.C., Hall, M.E. and Pollard, T.D. (1999) Proc. Natl. Acad. Sci. USA 96, 3739–3744.
[19] Rohatgi, R., Ma, L., Miki, H., Lopez, M., Kirchhausen, T., Takenawa, T. and Kirschner, M.W. (1999) Cell 97, 221–231.

[20] Blanchoin, L., Amann, K.J., Higgs, H.N., Marchand, J.B., Kaiser, D.A. and Pollard, T.D. (2000) Nature 404, 1007–1011.
[21] Marchand, J.B., Kaiser, D.A., Pollard, T.D. and Higgs, H.N. (2001) Nature Cell Biol. 3, 76–82.
[22] Hüfner, K., Higgs, H.N., Pollard, T.D., Jacobi, C., Aepfelbacher, M. and Linder, S. (2001) J. Biol. Chem. 276, 35761–35767.
[23] Linder, S., Nelson, D., Weiss, M. and Aepfelbacher, M. (1999) Proc. Natl. Acad. Sci. USA 96, 9648–9653.
[24] Higgs, H.N., Blanchoin, L. and Pollard, T.D. (1999) Biochemistry 38, 15212–15222.
[25] Sasaki, N., Miki, H. and Takenawa, T. (2000) Biochem. Biophys. Res. Commun. 272, 386–390.
[26] Krugmann, S., Jordens, I., Gevaert, K., Driessens, M., Vandekerckhove, J. and Hall, A. (2001) Curr. Biol. 11, 1645–1655.
[27] Zalevsky, J., Lempert, L., Kranitz, H. and Mullins, R.D. (2001) Curr. Biol. 11, 1903–1913.